Probing ALTAIR's Limits on Extended Objects

Brittney A. Cooper, Andrew W. Stephens, Christophe Clergeon, Adam Smith, John White, Laure Catala
Gemini North Observatory, 670 N Aohoku Pl, Hilo, HI 96720

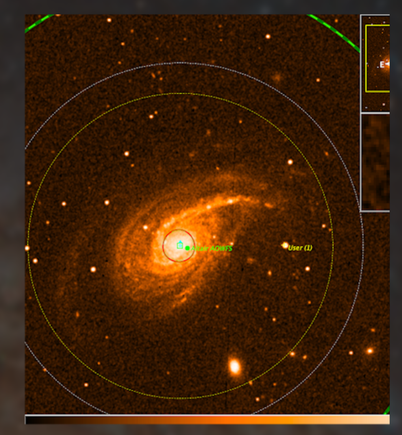

Background Image:International Gemini Observatory/NOIRLab/NSF/AURA
Image processing: T.A. Rector (University of Alaska Anchorage), J. Miller (Gemini Observatory/NSF's NOIRLab), M. Zamani & D. de Martin

ABSTRACT:

ALTAIR (ALTtitude conjugate Adaptive optics for the InfraRed) is Gemini North Observatory's natural/laser guide star adaptive optics (AO). ALTAIR transfers a corrected beam (1-2.5 microns) to Gemini Science instruments NIFS, NIRI, and GNIRS, reproducing the 8.1 meter telescope's focal ratio, pupil size, and position. ALTAIR has 3 main AO modes: a natural guide star mode (NGS; provides the best Strehl ratio), a laser guide star mode (LGS; poorer Strehl ratio), and a LGS mode where the LGS is combined with a peripheral wavefront sensor to increase the sky coverage for the tip/tilt natural guide star selection (super-seeing or LGS+P1; significantly decreased Strehl). Given the infrared bandwidth in which ALTAIR is usable, it is ideal for use on extended science targets such as galaxies, where dust and interstellar matter can obstruct observations in optical wavelengths. In AO, the distance of the bright tip/tilt guide star from the science target limits performance, so our goal is to better constrain limiting conditions and target parameters for successful on-axis extended object ALTAIR observations.This work revisits past extended object ALTAIR NGS and LGS attempts to create a pool of sample targets. The seeing conditions and tip/tilt guider counts from these attempts are recorded, and aperture photometry is performed on Hubble Space Telescope observations of the targets to determine the flux observed by Altair. The resultant brightnesses are converted to a standard R magnitude, and FWHM fits are run. The final goal is a cross-correlation of these values for observing scenarios where the NGS and LGS guide loops were successfully closed and stable, versus the scenarios where they were not. These results can then be used as more robust guidelines on limiting observing conditions, target aperture R magnitudes, and FWHMs for future Gemini proposals.

METHODS:

Past ALTAIR LGS and NGS extended object attempts can be identified via searches in the Gemini Observatory Archive, and ten targets were selected as a sample for both NGS and LGS. Next, Hubble Space Telescope (HST) Wide Field Planetary Camera 2 (WFPC2) calibrated fits files were obtained from the MAST Archive for each of the targets, to investigate their intrinsic characteristics independent of atmospheric effects. A script called "apphot.py" was created to streamline the process of performing aperture photometry and profile analyses on the HST data:

1) The image is processed to remove cosmic rays using LACosmic (van Dokkum, 2001).
2) The image is displayed (ex. Figure 1a) and the user is prompted to click on the center of the target.
3) The DAO Starfinder algorithm (Stetson 1987) runs with user-input coordinates to identify the center of the target. If it fails (usually due to asymmetry, large FWHM, or an inaccurate "threshold" parameter), the user is prompted to manually select the center.
4) An aperture photometry algorithm is run to capture the flux of the target through the Altair aperture radius of ~0.55":
- **a)** Image counts are multiplied by the fits "photflam" header keyword and divided by the exposure time to be converted to flux [erg/cm^2/A].
- **b)** The aperture background is averaged along an 0.05" annulus against the inner edge of the aperture.
- **c)** The background is subtracted from the remaining 0.5" of flux, and the subtracted flux is summed within 0.5" (Figure 1b).

5) The profile of the target is fit to a 2D Moffat profile using a vertical and horizontal cross-section of the target within the aperture. The FWHM of the Moffat is calculated. If a 2D Moffat fit is unsuccessful, a 1D Moffat fit of the average of the cross-sections is used.
6) The aperture flux is converted to an HST filter magnitude using the header photometric zeropoint.
7) The filter magnitude is then converted to a Johnson-Cousins R band magnitude using the python "synphot" (Lim, et al. 2016) package, with an elliptical source spectrum.
8) The script outputs the FWHM, the summed flux, the filter magnitude, and the R magnitude.

Figure 1: Panel a) depicts the HST images (36"x36") of the 20 extended targets sampled for this investigation. Panels b) and c) display the respective aperture and profile plots of the objects in panel a). Panel b) shows a cropped log-normalized field around the center of the target, with a red 0.5" aperture and white 0.05" background annulus. Panel c) overlaps an interpolated Moffat fit, 2 aperture cross sections, their mean, and the Moffat FWHM.

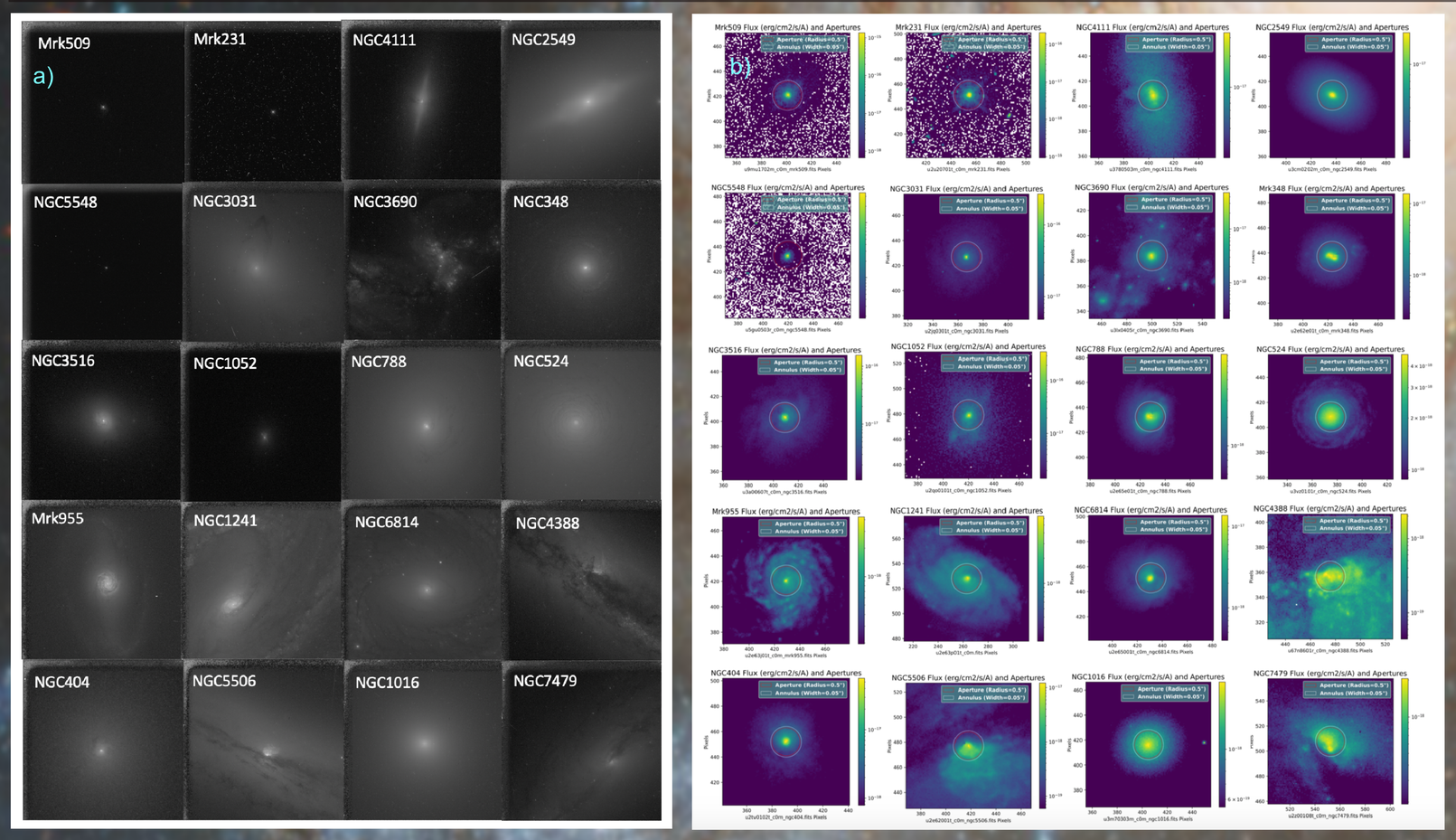

LGS Target	core FWHM (arcsec)	core R mag	Gemini Program ID (for ref)	observation date	avg natural seeing (arcsec)	STRAP avg guide counts (per subap) (LGTTCNTS/4)	LGTTEXP (ms)	Counts/ms	limiting R mag	Notes
Mrk 955	0.212	18.489	GN-2019B-FT-101	2019-10-27	0.55	22.5	5	4.5	21.429	Has an SFO tuning but looks like it was ignored. Obs were successful with target as TTGS and SFO before conditions degraded.
NGC 1016	0.733	18.07	GN-2013B-Q-29	2014-09-05	0.45	50	5	10	21.877	LGS, separate SFO star (left open)
NGC 2549	0.373	15.99	GN-2007B-Q-21	2008-03-29	0.65	250	10	25	20.792	LGS, separate SFO star (left open)
NGC 3690	0.263	15.718	GN-2011B-Q-73	2012-01-29	0.5	100	5	20	20.278	Used STRAP mag 15 on galaxy core, separate SFO star (left open)
NGC 4111	0.726	15.059	GN-2019A-LP-8	2019-05-09	0.4	50	1	50	20.614	LGS, separate SFO star (left open)
NGC 4388	0.467	17.943	GN-2015A-Q-3	2015-07-06	0.70	90	20	4.5	20.883	LGS, separate SFO star (left open)
NGC 524	0.882	16.66	GN-2007B-Q-21	2007-11-20	0.8	112.5	5	22.5	21.348	LGS, separate SFO star (left open)
NGC 5506	0.223	16.709	GN-2015A-Q-3	2015-07-01	0.70	55	5	11	20.620	LGS, successful obs on target nucleus
NGC 7479	0.881	17.737	GN-2010B-Q-25	2010-10-17	0.30	10	50	0.2	17.297	LGS, failed: object too faint for STRAP (couldn't close loops), estimating exposure to be max for STRAP and counts to be <15 (unstable)
NGC1241	0.334	17.789	GN-2019A-Q-106	2019-10-23	0.35	38	5	7.6	21.298	LGS, SFO on object
NGS Target	**core FWHM (arcsec)**	**core R mag**	**Gemini Program ID (for ref)**	**observation date**	**natural seeing (arcsec)**	**AO NGS guide counts (per subap)**	**AO EXP (1/AOFREQ) (ms)**	**Counts/ms**	**limiting R mag**	**Notes**
Mrk 231	0.214	14.358	GN-2018A-Q-112	2018-12-08	0.7	150	10	15	16.303	NGS on axis
Mrk 348	0.336	16.389	GN-2018B-Q-109	2018-08-30	0.85	20	10	2	16.147	Binary nucleus. NGS on axis, failed because guiding with 20 counts at 100 Hz and CFHT seeing tower reports seeing ~0.6-0.9 arcsec around the time of the observation.
Mrk 509	0.149	13.375	GN-2013A-Q-40	2013-07-06	0.40	100	5	20	15.633	NGS on axis, with field lens.
NGC 1052	0.169	14.125	GN-2018B-Q-109	2018-11-21	0.65	70	10	7	15.243	NGS on axis
NGC 3516	0.203	14.905	GN-2015A-Q-3	2015-05-26	0.60	85	10	8.5	16.234	NGS on axis, looks like trouble in seeing >> IQ20, all passed though.
NGC 404	0.29	15.317	GN-2018B-Q-109	2018-08-18	0.6	65	10	6.5	16.354	NGS on axis
NGC 5548	0.15	14.823	GN-2012A-Q-57	2012-04-04	0.90	90	20	4.5	15.461	NGS on axis. Able to close the loop in CC=70 at 50 Hz with about 125 counts.
NGC 6814	0.188	15.937	GN-2013B-Q-5	2014-09-01	0.40	95	10	9.5	17.386	NGS on axis. Lost guiding when seeing degraded (but many successful observations in good seeing).
NGC 788	0.48	16.576	GN-2018B-Q-109	2018-09-09	0.6	20	20	1	15.581	NGS on-axis, failed as unable to guide on galaxy nucleus even with 0.6" seeing and 50Hz.
NGC3031	0.156	14.674	GN-2014B-DD-7	2014-12-08	0.65	100	5	20	16.932	NGS on axis.

Table 1: LGS and NGS target aperture analysis results, Gemini observation parameters, limiting magnitude and observation notes.

RESULTS:

The results from the HST analyses can be used in conjunction with the measured AO seeing, and AO counts divided by the exposure of NGS/LGS tip/tilt (TT) wavefront sensor (WFS) from the attempted Gemini observations. They are reported in Table 1a and 1b for LGS and NGS, respectively. Given the maximum exposure time of the NGS and LGS TT WFSs and the minimum counts needed for enough signal to close the guide loops (2 counts/ms for NGS and 0.3 counts/ms for LGS), a "limiting magnitude" can be determined for each object. This value was determined and displayed in Table 1, however a larger data sample will be needed to observe useful correlations between it and aperture FWHM, magnitude and AO seeing. There is also a range of less ideal counts/ms where guiding is unstable, but not impossible in good conditions (2-5 counts/ms for NGS and 0.3-1 counts/-ms for LGS, as seen in Figures 2a and b). These ranges are approximate and based on anecdotal operations experience and failed or abandoned observations. In the case of LGS, it should be noted that most of the observations investigated operated with an open focus loop where a nearby star was used to tune Altair's slow focus offset and this is left out of the loop during the extended object observation. These instances are noted in Table 1.

Figure 3a displays the measured NGS seeing of the target with respect to its HST aperture FWHM, and the marker colors correspond to the HST aperture R magnitude. Figure 3b displays the same, but with aperture magnitude and FWHM swapped on the z and x axes. The corresponding parameters for the failed data delineate an approximate boundary for acceptable aperture magnitude and FWHM with respect to seeing. This boundary is approximated with a linear equation between the failed target and its adjacent passing target, and was used to make Table 2. For LGS (as NGS), there was no observed relationship of the aperture FWHM and magnitude with respect to seeing. Total counts appear to be the biggest constraint for the LGS TT, and the relationship between aperture FWHM and magnitude was used to generate an LGS table independent of seeing, also displayed in Table 2.

The current guidelines for NGS extended object observations are FWHM<0.6", however we found that a smaller FWHM (<0.3") is needed, and further investigations with more targets are required to verify a correlation with respect to seeing. We also found that an aperture R magnitude of <16 is required. For LGS, the current guidelines are for FWHM<1" and R magnitude approximately 1 magnitude brighter than the limits for point sources (with maximum R<18.5 in SB50). Sky brightness was not considered in this investigation but is another contributing factor and will be investigated in the future. Our results show that for an extended object in any LGS seeing conditions, the aperture FWHM should be <=0.9" for targets with an R aperture magnitude <18, and that fainter objects with aperture magnitudes 18-20 can be observed with a maximum aperture FWHM of 0.6".

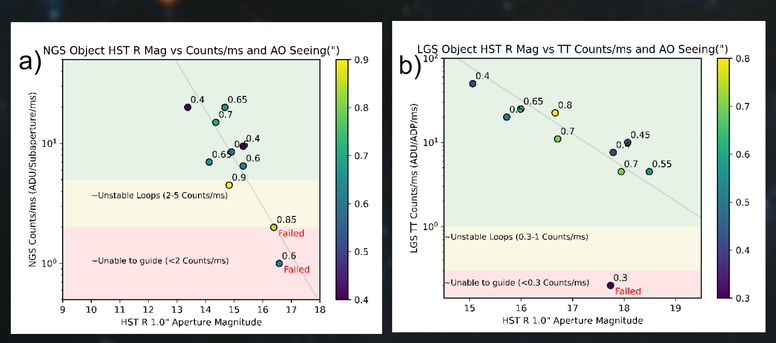

Figure 2: NGS (panel a) and LGS (panel b) targets plotted HST aperture R magnitudes compared to the counts/ms, with AO seeing as the colour axis. The limiting and unstable counts/ms ranges are color-coded and labeled. The black line in each plot represents the expected slope relating magnitude and flux.

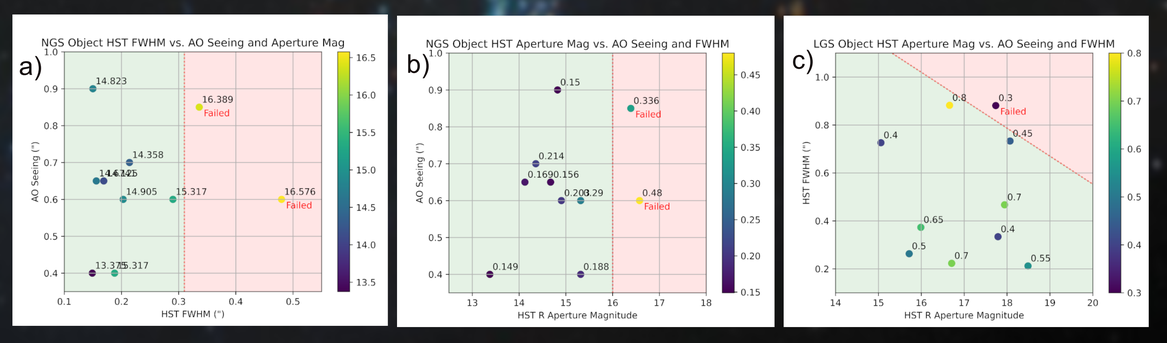

Figure 3: Panel a) displays NGS AO Seeing vs. aperture FWHM for successful and failed data, with aperture R magnitude as the color. The red line deliniates the approximate boundary of FWHM for AO Seeing combinations for a successful observation. Panel b) displays the same as Panel a), but with aperture FWHM and magnitude swapped between the color and x-axes. Panel c) displays the aperture FWHM with respect to aperture magnitude for LGS targets, as there was no correlation with AO seeing (shown in the color axis), along with the boundary between successful and failed observations.

	Seeing	Ap R Mag	Ap FWHM(")
NGS	<1.0	<16	<0.3
LGS	<1.0	<14-18	0.9
		18-20	0.6
NGS	<=IQ85	<16	<0.5
LGS	<=IQ85	<14-18	0.9
		18-20	0.6

Table 2: NGS and LGS resultant guidelines for aperture R magnitude and aperture FWHM of targets for seeing and Gemini conditions constraint bins.